Pergamon

Chaos, Solitons & Fractals Vol. 7, No. 4, pp. 523–541, 1996

0960-0779/96 $15.00 + 0.00

0960-0779(95)00091-7

Self-organized Criticality in Rainforest Dynamics

SUSANNA C. MANRUBIA and RICARD V. SOLÉ

Complex Systems Research Group, Departament de Fisica i Enginyeria Nuclear, Universitat Politècnica de Catalunya, Sor Eulàlia d'Anzizu s/n. Campus Nord, Mòdul B4-B5, 08034 Barcelona, Spain

(Accepted 11 September 1995)

Abstract—The dynamical properties of a cellular automata model of forest growth are studied. It is shown that fractal and multifractal structures, as well as power-laws (linked to both spatial and temporal variables) are generated, involving the appearance of a self-organized critical state. An extensive study of a real rainforest has been performed, and it is found that the model recovers very well the results of the real case. Some theoretical consequences are outlined.

1. INTRODUCTION

Cellular automata (CA) models have been used in recent years to recreate several aspects of a wide spectrum of complex systems. They are used as an alternative to a detailed description of a system, and it often proves to be enough to account for the main properties of it. CA are described by means of a lattice (where elementary automata are placed) and some rules of interaction on a local scale are defined. The system is updated in discrete time steps, either in a synchronous or an asynchronous fashion. A large class of these automata are able to drive themselves to a critical state with a wide range of length and time scales [1]. This is a self-organized critical state (SOC), which is characterized by free scale phenomena, both in time and in space. It proves to be an attractor for the dynamics.

Well known examples of cellular automata model that exhibit SOC properties are the pile of sand [2], the game of life [3] or the forest fire [4]. Although these models represent oversimplifications of real systems, it has been postulated that critical states could be widely present in nature. Although a critical point is usually a singular state of physical systems, where the system can be held by tuning some external field, it is conjectured that it might be the natural state for a biological system. This property would also make models plausible. Due to the absence of a characteristic scale in the phenomenon described, a simple model that skips the smallest details is suitable to reproduce the real dynamics. A key property of living systems is their capability to evolve. Evolutionary processes lead to changes in the interactions among individuals and as a consequence, different dynamical regimes can be explored. In this sense, it has been conjectured that critical states are a necessary requirement for evolvability [5]. Systems that display SOC may be the most robust and well adapted to external perturbations, and the real evolution under biological constraints would lead unfailingly to such states. In recent years it has been shown that SOC is a physical process involved in many real systems, from earthquakes [6] to large scale evolution [7].

In this paper we analyse the behaviour displayed by a CA model of tree growth and death. We call it the Forest Game (FG) [8]. The model exhibits the properties of self organization in a critical state (power-law distributions) and self-similar spatial patterns.

Temporal scale fluctuations in biomass present a $1/f$ noise, a fingerprint of SOC. We compare the obtained results with a real rainforest: Barro Colorado Island (BCI), in Panama. This particular case is studied using the multifractal formalism and some other tools from the theory of critical phenomena. The real forest is identified with a particularly interesting place of the parameter space of the model, exactly where a critical transition takes place.

In Section 2, the multifractality of BCI is analysed. The spectra of generalized dimensions and correlation functions are calculated, as well as the spatial correlation function and some other physical quantities that are shown to follow power-law distributions. In Section 3, we present our model, the Forest Game, and analyse the dynamical evolution and spatial patterns that the model is able to generate, as a function of some key parameters. At the end of the section, we compare the real and the simulated forest: this is evidence of a real ecosystem self-organized in or close to a critical point. In Section 4, we discuss the implications of our results and outline the future research in this field.

2. BARRO COLORADO ISLAND

2.1. *Multifractal measures*

SOC involves the generation of spatial patterns with self-similar properties. Often (and in particular for ecosystems) only a spatial snapshot of the underlying dynamical state is available. The snapshot can be informative if an adequate set of statistical measures is used. Multifractal calculus allows us to extract the maximum information.

In 1974, Mandelbrot introduced the concept of a multifractal when he was working in the context of the turbulence. Fractals were already well known and understood objects, and accepted to be widely present in nature. Since then, multifractal calculus has been rigorously developed and successfully applied to many different fields. The basis for the systematic calculus of multifractal function is Halsey *et al.* [9]. Multifractal properties have been described for different systems: river models [10], networks [11], strange attractors [12] and binomial measures [9], among others.

In order to perform a multifractal calculus, a measure needs to be defined over the d-dimensional system Ω, where a measure $\mu(\mathbf{x})$ is assumed to exist. The total size of the set must be normalized to one, and then, it should be partitioned into $\{B_i\}$ $i = 1, \ldots, n$ pieces of length l_i. A probability measure p_i is assigned to every piece, i.e.,

$$p_i = \int_{B_i} \mathrm{d}\mu(\mathbf{x}). \tag{1}$$

If Ω is a multifractal object, then it can be described as $\Omega = \bigcup_\alpha \Omega_\alpha$, where $\{\Omega_\alpha\}$ are subsets with scaling $p_i \sim l_i^\alpha$. Following Ref. [9], a partition function is defined,

$$\Gamma(q, D(q), \{B_i\}, l_i) = \sum_{i=1}^{B_n} \frac{p_i^q}{l_i^{\tau}(q)} = 1, \qquad q \in \mathcal{R} \tag{2}$$

where

$$\tau(q) = D(q)\,(q - 1) \tag{3}$$

with the only requirement being the normalization of the measure

$$\sum_{i=1}^{B_n} p_i = 1. \tag{4}$$

Equation (2) gives an implicit definition of $D(q)$. In the particular case of $l_i = l$, $\forall B_i$, $D(q)$ can be explicitly written, and one gets

$$D(q) = \lim_{l \to 0} \left\{ \frac{1}{q-1} \frac{Ln\chi(q)}{Lnl} \right\}, \tag{5}$$

where $\chi(q) = \sum_i p_i^q$. $D(q)$ are called correlation dimensions. The complete spectrum of fractal dimension for the set can be obtained through

$$\alpha(q) = \frac{\partial}{\partial q}[(q-1)D(q)] \tag{6}$$

$$f(\alpha) = q(\alpha) - [q(\alpha)-1]D(q(\alpha)) \tag{7}$$

where $f(\alpha)$ represents the fractal dimension of a set that has a diverging exponent α in the measure.

The function $\tau(q)$ behaves as a straight line in the limit $q \to \pm\infty$, and its asymptotes give the values of the end points of the $f(\alpha)$ spectrum. It can be seen that $\tau(q)$ satisfies the following limit conditions:

$$\lim_{q \to -\infty} \tau(q) = \lambda q - e \tag{8}$$

$$\lim_{q \to \infty} \tau(q) = \bar{\lambda} q - \bar{e} \tag{9}$$

with $\lambda = \alpha(+\infty)$, $\bar{\lambda} = \alpha(-\infty)$, $e = f(\alpha(+\infty))$ and $\bar{e} = f(\alpha(-\infty))$ [13].

2.2. *The multifractal rainforest*

The real system that we studied is a tropical rainforest located in Barro Colorado Island, isolated and preserved after the construction of the Panama canal. In Fig. 1(A) a map of 50 hectares (1 ha = 10^4 m^2) of BCI is represented. It is a quite flat and wild terrain in the central part of the island [14]. This apparently simple map was possible after two years of field studies in the island, and was drawn using measures from the ground. There 2582 low canopy survey points are shown as black dots. They indicate that the height of the canopy was ≤ 10 m in 1982, 1983 or in both years. These low canopy points represent the recent formation of a clearing, due to treefall. It is known that clearings are responsible for the great diversity found in tropical rainforests: different species have different needs of light, space and nutrients, and hence the existence of clearings of many sizes allows the coexistence of many species. On the other hand, there is a dynamical counterpart to the spatial distribution of trees: the continuous generation of clearings allows new individuals to develop, and the evolution and competition among individuals in the rainforest continues [15].

To estimate the fractal dimension of the forest the picture was transformed into a binary matrix. A value 1 was assigned to black sites, and 0 to white ones. A computer program counted the occupied boxes having sizes between 1×2 (or 2×1) and 10×10, in plot units. The system was covered by rectangular and square boxes, in the vertical and in the horizontal direction, and all integer box sizes were used. The whole plot has size 100×200 in these units, and each pixel represents a surface of 5×5 m^2 in the real forest. Figure 2(A) shows the results. The existence of a fractal dimension for the set is apparent with a continuous drift of the fractal dimension below a distance $d_1 \simeq 30$ m in the real forest. This continuous decrease in D_0 has been already noticed by some authors. A concave log–log graph has been often found, mainly related to biological systems (lungs, leaves and contours of cells, among others) when observed in a deeper scale (compared to the length

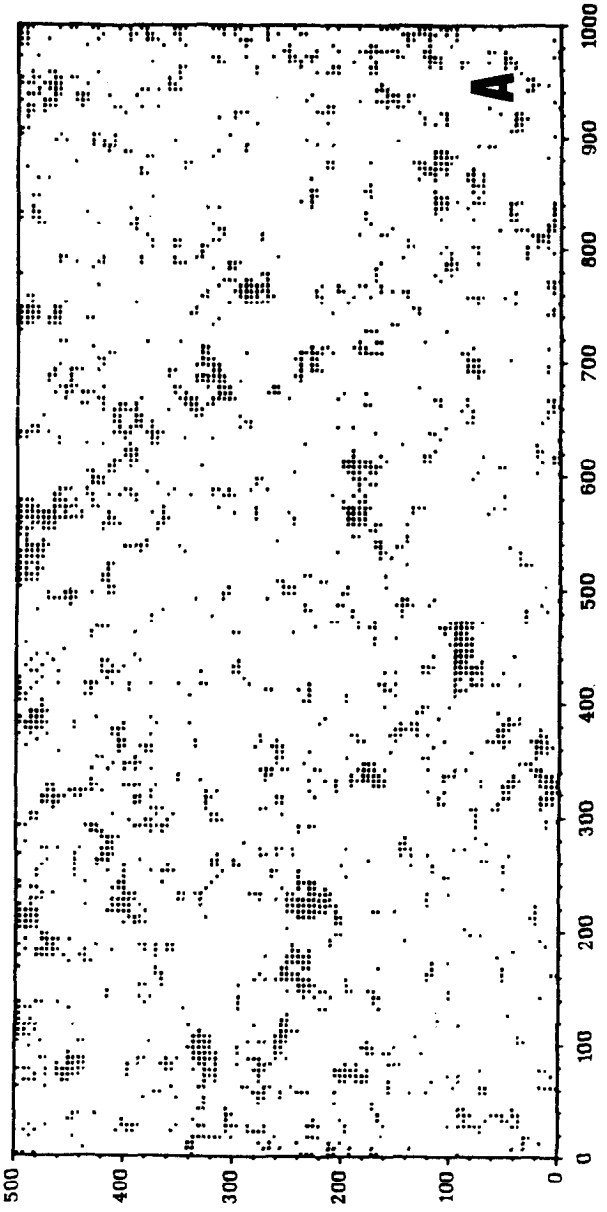

Fig. 1(A). *Caption opposite.*

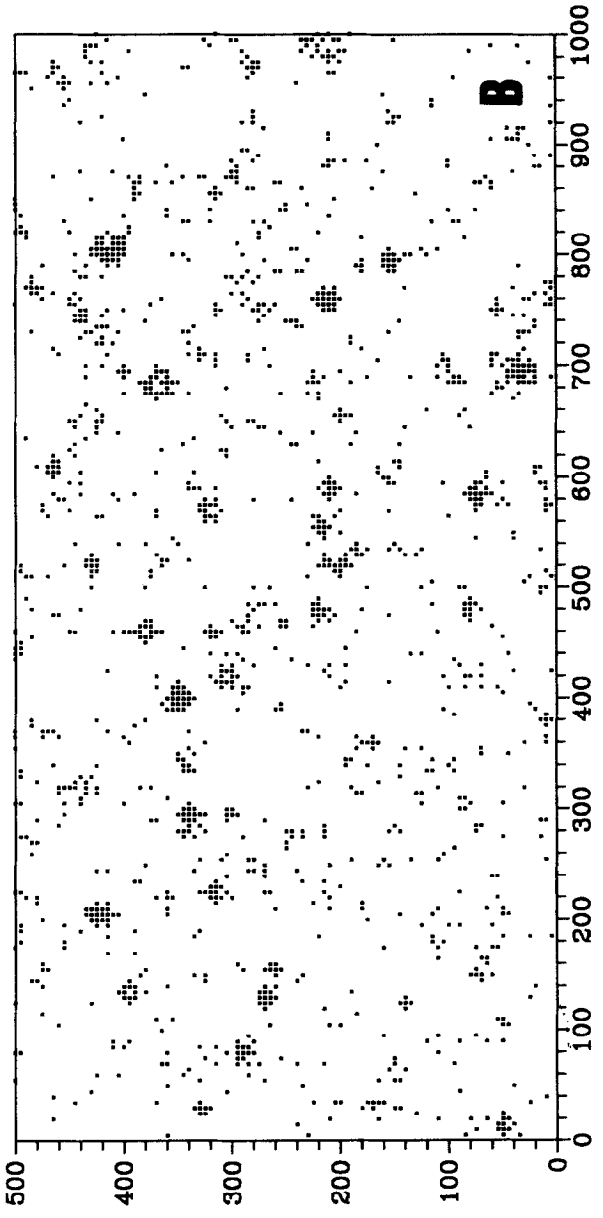

Fig. 1. (A) Snapshot of the 50 ha of Barro Colorado Island, a tropical rainforest in the Panama canal area. Black points represent those places where the canopy was lower than 10 m in 1982, 1983 or in both years, due to recent treefall; (B) snapshot produced by the forest game in a 100×200 lattice after 200 time steps. There is a striking similarity with the former real pattern.

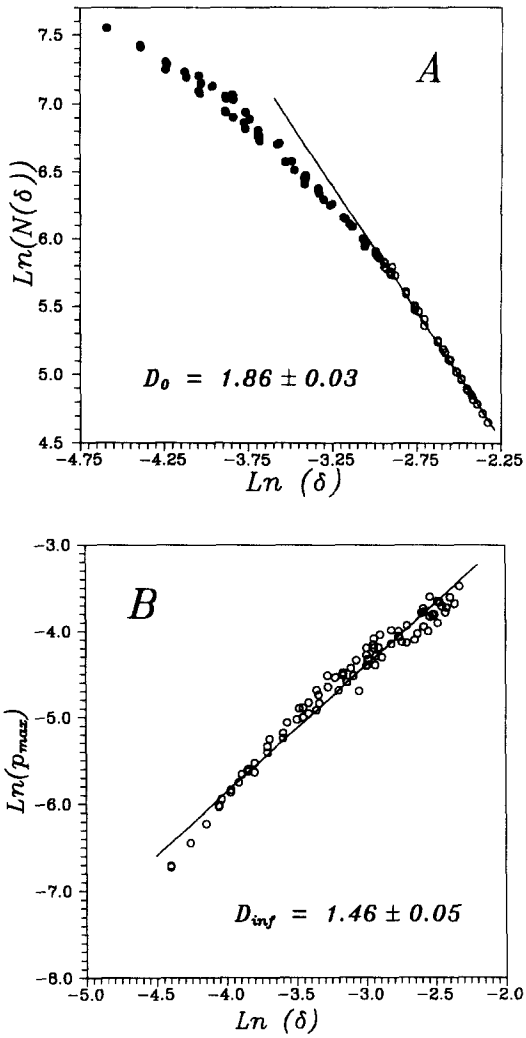

Fig. 2. (A) Box-counting carried out over the set of Fig. 1(A). Notice the continuous drift in D_0, pointing out the underlying multifractal structure; (B) box-counting for the maximum probability in the same set, in order to obtain the value of $D(\infty)$.

scale at which any structure would disappear). Real systems with fractal properties show a progressive change of D_0, rather than a cut-off until which the system fits a straight line (in a log–log plot). This existence of several successive structures, reflected in the gentle change in D_0, constitutes evidence for multifractal scaling [16].

We estimated the fractal dimension for d between 30 and 60 m in the real forest. This is clearly the part of the graph where the linearity is evident. The fractal dimension of the forest in this range is $D_0^{BC} = 1.86 \pm 0.03$. Over a characteristic length of $d_2 = 60$ m for the boxes, one cannot find any empty box. The non-trivial self-similarity is lost and the fractal dimension becomes 2[†].

[†]Although this distance is perhaps too short to talk about a fractal distribution of clearings (that would be rigorously obtained only at a percolation point) it will be shown that the distribution of sizes (areas) of clearings vs relative frequency of every size fits a power-law. This is only a first evidence. What really tells us that the rainforest is evolving close to a critical point is the self-similarity of the biomass distribution.

It is known that the asymptotes of $D(q)$ can be easily obtained if one knows the values of the extreme probabilities of the boxes of the set:

$$D_{\infty} = \frac{Ln(p_{\max})}{Ln(\delta)} \tag{10}$$

$$D_{-\infty} = \frac{Ln(p_{\min})}{Ln(\delta)} \tag{11}$$

for every scale δ. It is clear that D_{∞} and $D_{-\infty}$ should be calculated by performing a linear regression, as is usually done for D_0. The second calculation we carried out was D_{∞}, the correlation dimension for $q \to \infty$, and we used the same range of distances as in the previous one: see Fig. 2(B). The interpolation was made using all the points, and the result was $D_{\infty}^{BC} = 1.46 \pm 0.05$. The obvious difference between D_0^{BC} and D_{∞}^{BC}, as well as the observed continuous drift in D_0^{BC}, are strong arguments supporting multifractality. In our case, it was impossible to do the same with $D_{-\infty}$, due to the size of the real system. In the available domain of lengths, $p_{\min}$ keeps almost constant, so $D_{-\infty} \approx 0$. But, as $D_{-\infty} > D_0 > D_{\infty}$, it cannot be accepted as a measure of $D_{-\infty}$. Therefore, the calculation will try to adjust the left side of $D(q)$ as well as possible, and some discrepancies could arise in the right side. There can be found different optimizing methods to choose the scale at which one should define the measure to perform the multifractal calculations [17]. We believe that, in this case, the adjustment of D_0 and D_{∞} is enough to choose δ in a right way.

The measure defined on our set is a mass measure. Every black pixel is assigned a probability $p_d = 1/N_P$, where $N_P = 2582$ is the total number of black dots in the forest. The box size that best fits the calculated D_0 and D_{∞} is a 4×4 box, again using the pixels as elementary distance units.

We are dealing with a set of points distributed over a lattice. Once the size of the box is chosen, it is particularly easy to calculate $\tau(q)$, $D(q)$ and $f(\alpha)$ according to expressions (3), (5)–(7). Let us define N_j as the total number of boxes containing j low canopy points. The selection of 4×4 boxes implies that j takes a small number of discrete values, from 0 to 16. Now we can write $\chi(q)$ as

$$\chi(q) = \sum_j N_j \left(\frac{j}{N_P}\right)^q. \tag{12}$$

The sum over boxes ($\sim 10^3$) transforms into a sum over occupation numbers ($\sim 10^1$). The multifractal functions obtained for BCI can be seen in Fig. 3. First of all, the $\tau(q)$ spectrum (Fig. 3(A)) is depicted. Its asymptotes give the end points of the spectrum of multifractal dimensions (according to (8) and (9)) and its values are represented in Fig. 3(C), together with the slope-one tangent to $f(\alpha)$. $f(\alpha(\infty))$ and $f(\alpha(-\infty))$ give a non-zero value. This is due to the non-zero measure of the set supporting the extreme probabilities in the distribution function that is found. This distribution is very close to an exponential one, but there is an obvious cut-off at the size 16 (the maximum occupation number).

2.3. *Critical properties*

The fractal patterns that have been found in BCI may be a fingerprint of a system in a critical state. The image is quantified by a power-law function. Fluctuations in the variables of the system change in such a way that they present a wide spectrum of sizes, from very small to the maximum allowed size, and they follow a power-law. The appearance of universality in systems close to a critical point is another essential property. Some

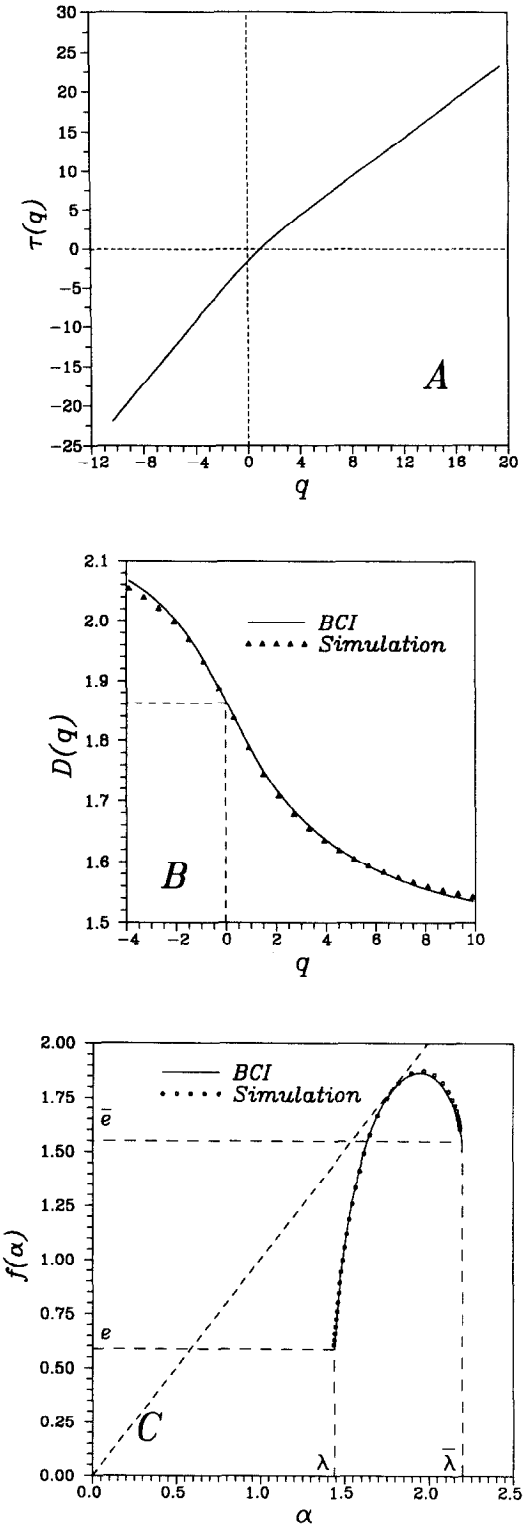

Fig. 3. Multifractal functions for BCI and a simulation for some given parameters (see main text). (A) $\tau(q)$. The asymptotes of this function were evaluated to be $\lim_{q\to\infty} \tau(q) = 1.44q - 0.59$ and $\lim_{q\to-\infty} \tau(q) = 2.20q - 1.55$; (B) spectrum of correlation dimensions for a real and a simulated forest; (C) $f(\alpha)$ spectrum for BCI and a simulation, using the same parameters as those in (B).

quantities can be defined (the critical exponents) and their values are common to different classes of systems that follow a few very general assumptions. In this section, we present additional results that help to corroborate the conjecture that BCI is actually a large living multifractal with critical dynamics.

When observing a tropical rainforest, we are faced with a highly nonlinear dissipative system. The dynamical evolution of such a system is mainly led by the continuous creation of clearings. They leave places for new trees to be grown, and the size of the open canopy is a key element in the selection of which species becomes established there. This is why a study of the distribution should prove useful in order to understand the underlying dynamical laws.

Hence, first of all, we calculated the frequency distribution of gap sizes in the BCI map. There is a well defined power-law, as can be seen in Fig. 4(A):

$$N(G) \propto G^{-\xi} \tag{13}$$

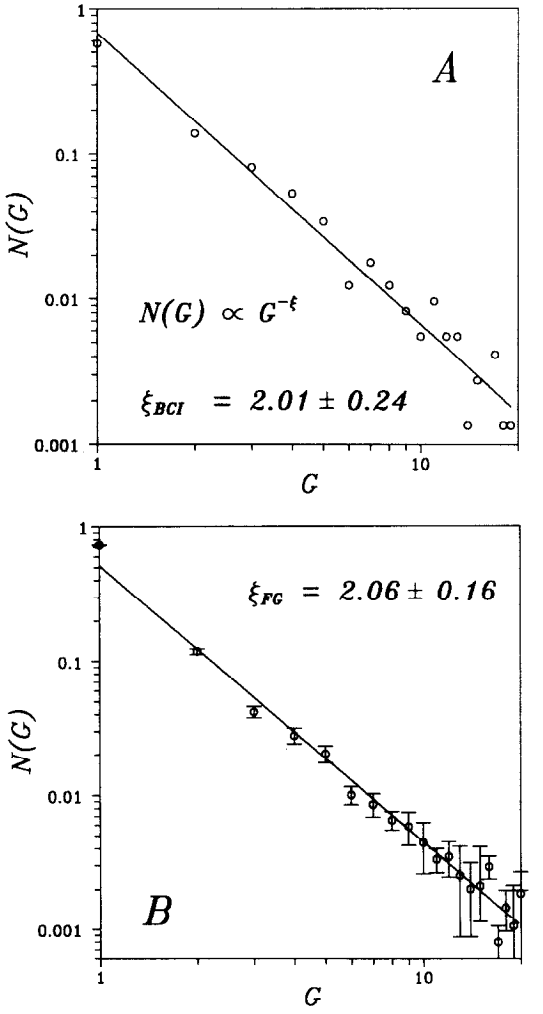

Fig. 4. (A) Power-law scaling of cluster gap sizes in BCI. Two points are considered to belong to the same cluster if they are side-by-side. Points connecting through the corners belong to different clusters. Other elections of neighbourhood do not affect the power-law distribution; (B) the same measure made over the model, with $P_d = 0.013$ and $\gamma = 2.5$. Ten independent runs of 200×200 lattices have been averaged, after 200 transients were discarded.

with $\xi = 2.01 \pm 0.24$. The biggest gaps are omitted from the figure ($G = 37$, 39, 52 and 90, one of each). It is our belief that this has a different generating mechanism than the simple falling of trees, say external disturbances. The role of these large clearings is discussed later. The maximum cluster size fitting the power-law is $S_M = 27.4m \approx d_1$. The correlation function was also calculated for BCI data, and this is shown in Fig. 5(A). It is calculated as the average in the number of neighbours (N_n) at a distance d ($d = |\mathbf{r} - \mathbf{r}'|$) with $\mathbf{r}$ and $\mathbf{r}'$ the positions of a point and its neighbours, respectively, from a given black site. The sum is performed over all the black pixels that lie at a distance d_b from the boundaries such that $d_b \geq d$ [18]. The total number of pixels verifying this is $N_P(d)$. The normalizing factor N is $N_P(d)$ times the maximum number of neighbours ($N_n^{\max}$) at that distance:

$$C(d) = \frac{1}{N} \sum_{|\mathbf{r}-\mathbf{r}'|} \rho(\mathbf{r})\rho(\mathbf{r}') \tag{14}$$

$\rho(\mathbf{r}) = 1$ for a black site, and 0 for a white one.

The correlation function reveals three well-defined parts. The first one runs from the

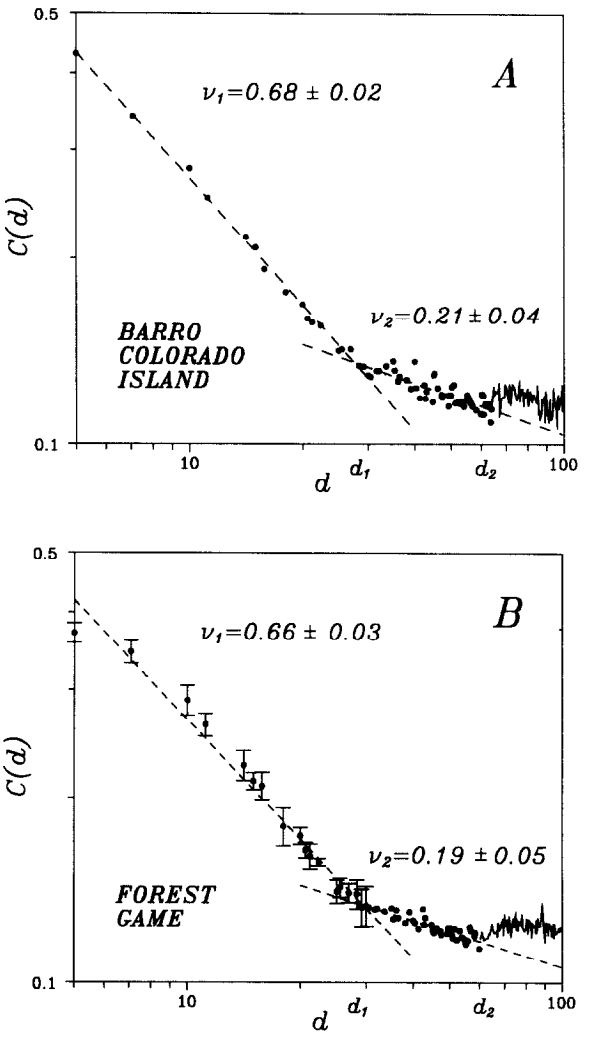

Fig. 5. (A) Spatial correlation function for BCI; and (B) for the simulated forest, where five runs of 200 × 200 lattices have been averaged. In the simulation, $\gamma = 2.5$ and $P_d = 0.013$.

closest neighbours (at a distance of 5 m in the real forest) to $d_1 \simeq 30$ m. It scales as a power-law, $C(d) \propto d^{-\alpha}$, with $\alpha = 0.68 \pm 0.02$. The fractal dimension of a set is related to the exponent of the correlation function by $d = D_0 + \nu$, where d is the spatial dimension and $C(d) \approx d^{-\nu}$. In the first are described, $D_0 = 1.32 \pm 0.02$, according to the last expression, with $d = 2$ and $\nu = \alpha$ and this value is quite close to the averaged slope from the box-counting, $D_0^{BC} = 1.17 \pm 0.05$.

The second part corresponds to $30 < d < 60$ m, and it gives another well-defined power-law, $C(d) \propto d^{-\beta}$, $\beta = 0.21 \pm 0.04$. Now $D_0 = 1.79 \pm 0.04$, in quite good agreement with the calculated value $D_0^{BC} = 1.86 \pm 0.03$. Out of these two areas for $d > 60$ m, the fractal dimension of the forest becomes 2, as has been discussed, and $C(d)$ shows another sharp change. It is no longer a power-law function but keeps almost constant. Hence, there are two characteristic lengths, $d_1 = 30$ m, $d_2 = 60$ m, that point out the existence of phenomena taking place at different scales and with different results. In particular, d_2 can be thought of as the typical distance of connected biomass, without breaks produced by clearings. A careful observation of the spatial correlation function reveals a gentle increase in the value of $C(d)$. For $d > d_2$, there are no more changes. This distance is an upper limit value in the fractal behaviour of clearing size [19]. The change in the exponent of $C(d)$ also supports multifractality. The possible implications will be discussed in the last section.

The previous results have been obtained from a snapshot of a real rainforest. They provide evidence that BCI is a living system in or close to a critical state. In order to obtain further evidence of this conjecture, theoretical models can be extremely useful. Here a CA model will be used. This model can show us how these structures are formed and can also give us temporal dynamics, not available (at all) from field studies on forest dynamics. Given the enormous difficulty of getting such an amount of information (together with the years required to get it) the following model of rainforest dynamics was proposed in order to fill this lack.

3. THE FOREST GAME

3.1. *Cellular automata model*

The forest game (FG) [8], is a stochastic cellular automaton (CA) running on a two-dimensional $L \times L$ square lattice,

$$\Lambda(L) = \{(i, j) | 1 \leq i, j \leq L\} \tag{15}$$

with periodic boundary conditions. A CA is placed in every site. It can grow from a minimum size S_0 to a maximum height S_c. The rate of growth depends on the strength of the interaction with its neighbours. The dynamics of the model is based on the competition for resources among the trees. The internal state of every automaton (the height of every tree) is determined through a function $S(i, j)$, where $i, j \in 1, 2, \ldots, L$ represent its position in the lattice.

Four basic rules defined the automata.

(A) *Growth*. A given tree grows if the screening from its eight nearest neighbours is weak enough. The tree size is updated at every time step n according to the next rule:

$$S_{n+1}(i, j) = S_n(i, j) + \Delta_n(i, j). \tag{16}$$

$\Delta_n(i, j)$ includes the way in which nearest trees interact. We take a simple screening of the neighbours, and $\Delta_n(i, j)$ is defined as

$$\Delta_n(i, j) = \mu\Theta\left[1 - \frac{\gamma}{8}\sum_{\langle r, s\rangle} S_n(r, s)\right]. \tag{17}$$

$\Theta(z) = z$ if $z > 0$, and $\Theta(z) = 0$ if $z < 0$: if the screening is too high, growth is not allowed. $\langle r, s\rangle$ indicates the restriction to the eight nearest trees, and, obviously, $(r, s) \neq (i, j)$. We take $\mu = 1$ in all the simulations. γ represents the interaction strength, and it will be revealed as an important parameter in the dynamics of the model. If $\gamma = 0$ no interaction takes place (trees grow independently), and for $\gamma \to \infty$, growth becomes impossible.

Δ_n tries to introduce every kind of competition among trees: the race for light, for nutrients, for soil and the possible interaction with other plants or animals that might take a role in growth. Δ_n is quite a simple function, but if the rainforest, as a dynamical system, operates near a critical point, it is known that the scale invariance implies independence from the fine details of the model, and Δ_n has to be enough to catch the essential features of all interaction factors.

(B) *Death*. A tree will fall down when the maximum height S_c is reached. It can also die at any time according to some probability P_d that is kept fixed. Immediately after its death, the height of the tree is set to zero. Real data available from some rainforests support the ansatz that P_d roughly takes a constant value for any life-time of the tree. The probability of death has likewise been evaluated between 1 and 2% per year [20].

(C) *Clearing formation*. When a tree dies, a clearing in the canopy is formed. Not only is the dead tree removed, but also the nearest neighbours in a radius R according to the next rule:

$$\sum_{\langle r, s\rangle} S_n(r, s) \leqslant S_n(i, j), \tag{18}$$

where $((r - i)^2 + (s - j)^2 \leqslant i^2 + j^2)$. The mass of neighbours removed is proportional to the size of the falling tree, and at most equal to it. R is determined through the previous inequality. When the chosen tree falls down, only the biomass removed by this first tree is considered, and not the biomass that the neighbours that are eliminated by the first falling tree could also remove. This is a very reasonable rule that prevents the appearance of unbiological avalanches of the size of the system. This rule also moves the system away from an exact SOC state and brings about the appearance of a cut-off in some of the computed functions, as will be seen.[†]

(D) *Germination*. A new tree can appear at any empty lattice site with some probability P_b. The size of the new tree is the minimum one, S_0. We take $S_0 = 0.1$ in all our simulations.

The lattice is updated in an asynchronous fashion. At each time step $L \times L$ lattice sites are randomly chosen and, depending on the state of the automata, one of the previous rules is applied. The updating of the lattice was chosen in such a way that a time step is approximately equivalent to a year of evolution in a real rainforest.

As can be seen, only the main properties of what might be a real forest are included as the rules of the CA, and neither fine details about tree structure nor about interactions are considered, provided the system has a close-to-critical-state organization.

[†]Biological constraints must be taken into account. Neither arbitrarily large trees nor gaps can be formed in the real forest. Such types of constraints lead to a restricted capability of the system to reach critical states.

3.2. *Results*

In all the simulations performed, the probability of germination was kept fixed to a value $P_b = 0.5$, and the interaction strength γ and the probability of death P_d were chosen as parameters of the model. Even so, if one wishes to reproduce real non-perturbed rainforests, P_d has to be kept between 0.01 and 0.02, as stated in the last subsection. γ would really be the single free parameter of the model. It is not possible to make an estimation of it using data coming from real systems. In Fig. 6, the parameter space of the model is represented. Different choices of P_b simply shift the position of the domains that are to be described, but do not alter the different behaviours that the model displays. Three well-defined different areas were found.

3.2.1. Damped oscillations (DO). A small part of the parameter space presents damped oscillations in the biomass. Due to the small interaction and also to the small probability of death, trees start to grow simultaneously and at the same rate. They mostly die when the maximum size $S_c = 30$ is reached, and the birth and growth start again. Eventually, the system becomes uncoupled due to the small but non-zero probability of death and also because they do not appear exactly at the same time (the oscillation in the biomass is damped). The Fourier transform of biomass fluctuations has been also calculated. We used an average of eight runs of 2^{10} time steps and no transients were discarded, to make evident the periodic behaviour of the biomass. In this case it obviously presents a peak, produced by this oscillation, and no further structure is observed.

The distribution of tree sizes, $F(h)$ has also been measured. In all the calculated $F(h)$, 200 transients were discarded and 10 independent runs of 200×200 lattices were averaged. In the area of damped oscillations, the size of the trees at the nth time step can be obtained in analytic form. Consider equation (17), and let $\bar{s}$ be the average size of trees. For a small enough γ (as is the case in this domain), the growth at every time step becomes

$$\Delta = 1 - \gamma\bar{s} \tag{19}$$

where $\gamma\bar{s} < 1$ is assumed. Then, the size of a tree at the nth time step is

$$S_n = 1 + (1 - \gamma\bar{s}) + (1 - \gamma\bar{s})^2 + (1 - \gamma\bar{s})^3 + \ldots + (1 - \gamma\bar{s})^{n-1} + (1 - \gamma\bar{s})^n S_0. \tag{20}$$

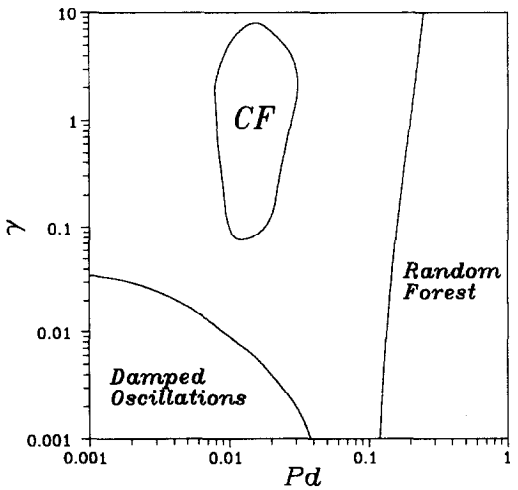

Fig. 6. Parameter space of the forest game. The marked domains are described in the main text.

The last expression can be added up, and we finally get

$$S_n = \frac{1}{\gamma\bar{s}} + \left(S_0 - \frac{1}{\gamma\bar{s}}\right)(1 - \gamma\bar{s})^n. \tag{21}$$

If $\gamma\bar{s} \ll 1$, then $\Delta \approx 1$, and only integer sizes (plus S_0) are allowed. If $\gamma\bar{s}$ is small but not negligible, the distribution of trees presents peaks at approximately integer sizes, 'modulated' by the delay produced by $\gamma\bar{s}$. Tree distributions can be seen in Fig. 7. When one gets closer to the boundaries of this area, the damping is increased, $\gamma\bar{s} \approx 1$, and the described structure fades away.

3.2.2. Random forest (RF). The right most part of the parameters space is termed random forest because of the almost independent way in which trees grow in this area. Now, it is not a result of an almost null interaction strength but is due to the absence of neighbours, since the probability of death is very high. It starts to grow, but it will soon die. In this area, the fractal dimension becomes 2, pointing out the almost random germination and death of trees. Some spatial structure is still observed when keeping close to the left boundary. This is reflected in the spreading of the multifractal functions, even with $D_0 = 2$. This partial spreading is lost when moving towards $P_d = 1$, and the whole multifractal spectrum collapses to a single value ($D(q) = 2$, $\forall q$, and $f(\alpha)$ becomes a single point). The distribution of trees obtained, $F(h)$, decays fast and big trees are seldom found (see Fig. 7(B)).

3.2.3. Complex forest (CF). The most interesting area of the parameter space is the central part termed complex forest. In this area, the Fourier transform ($P(f)$) of the biomass fluctuations, i.e., of $B(\Omega, t) = \sum_{\Lambda(L)} S_t(i, j)$ gives a spectrum $f^{-\phi}$, with $\phi > 0.85$. Figure 8 displays some of the obtained spectra in this phase. They were obtained with 2^{10} time steps after 200 transients were discarded, and an average was made over eight $N \times N$ lattices. This measure has been used to study possible finite-size effects. $P(f)$ was calculated for three different lattice sizes, and no important deviation in the power-law is found. Only for the smallest size ($N = 10$) a slight deviation in the higher frequencies is observed. Also the multifractal functions give a reasonable spreading of values (wider than in any other domain of parameter space) and D_0 is always non-integer. Some multifractal functions can be seen in Fig. 9. The spatial correlation function behaves as a power-law (Fig. 5(B)) and scaling laws for gap cluster sizes and for tree sizes are also found.

3.2.4. The white area (WA). This represents a transition among the three described domains. Partially fractal structures and weak correlations are found, as well as power-laws in biomass fluctuations that deviate more and more from $1/f$ noise. The distribution of trees changes from a clear power-law to an exponential distribution, while keeping close to CF. It starts to oscillate when approaching DO and decays fast when moving towards RF.

From the previous results, it can be seen that our CA model, the forest game, can display many different states of dynamical equilibrium. There is a domain in parameter space that generates self-organized criticality. But what about the real data? The already observed properties of the model seem to indicate that, at least qualitatively, BCI is well reproduced. And the place where real physical measures best fit belongs to the most 'complex' patterns that the model is able to generate. In particular, there is a combination of parameters, $P_d^* \approx 0.013$ and $\gamma^* \approx 2.5$ that recovers almost exactly all the functions and values measured in BCI. Figure 1(B) reproduces a snapshot of a 100×200 lattice for these

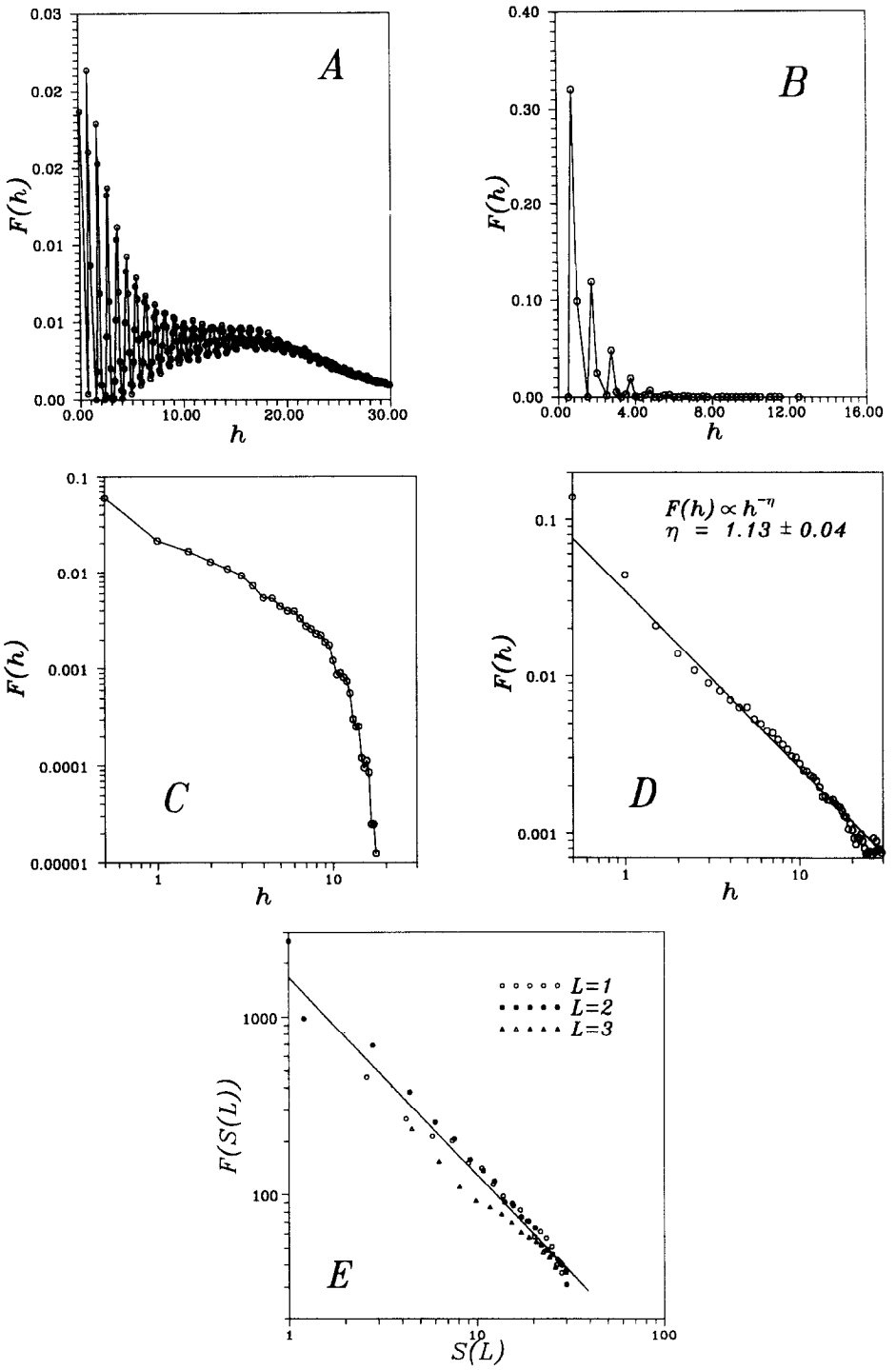

Fig. 7. Tree distribution given by the forest game. Many different functions can be found, depending on the chosen parameters. (A) $P_d = 0.001$, $\gamma = 0.01$, in the damped oscillations domain; (B) $P_d = 0.6$ and $\gamma = 0.1$, in the random forest area; (C) $P_d = 0.02$, $\gamma = 9$. Even a slight deviation from the complex forest domain produces an exponential-like distribution; (D) $P_d = 0.013$ and $\gamma = 2.5$. The power-law distribution is well-fitted, except in the smaller sizes, due to the existence of a minimum tree height; (E) space renormalization of tree size distribution for the parameters of (D). Two different block sizes have been used. Both fit quite well to the original distribution (continuous line).

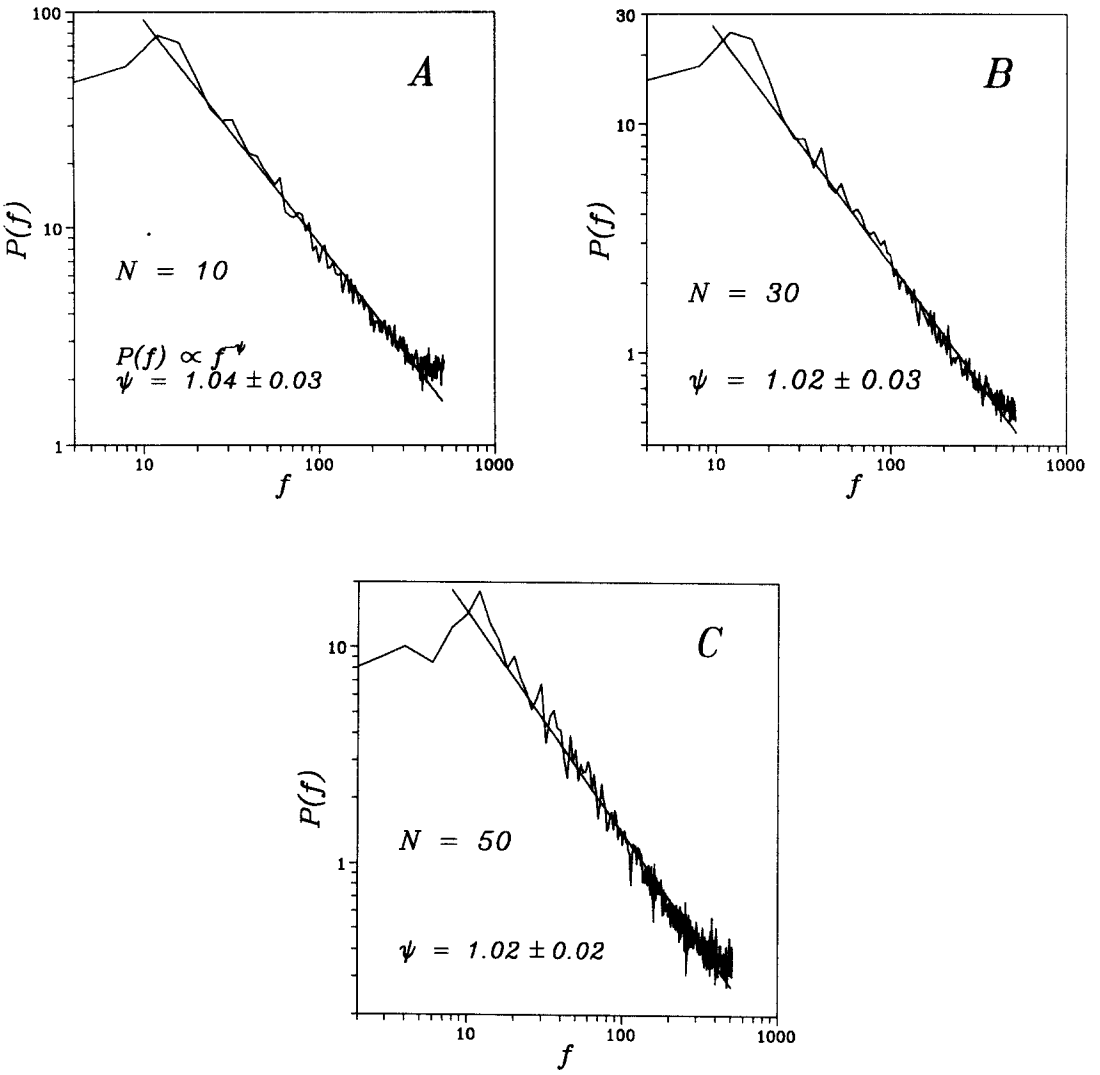

Fig. 8. Fourier transform of biomass fluctuations. Three different lattice sizes have been used (with the same parameter set) in order to evaluate possible finite-size effects. (A) $N = 10$; (B) $N = 30$; (C) $N = 50$.

parameters. In Fig. 3(B), (c) $D(q)$ and $f(\alpha)$ for BCI are plotted together with the ones obtained for the given parameters. In Fig. 5(B), the spatial correlation function is represented. It also shows the change in the slope at the same point that was found for BCI, and the exponents are the same within the error. Not only are the known values reproduced, but the model also allows the prediction of other results of real rainforests presenting such spatial patterns: P_d^* and γ^* give a Fourier transform of biomass fluctuations with $\phi = 1.02 \pm 0.03$, which is the closest to $1/f$ noise in our parameter space. Also a power-law scaling of tree sizes and of gap sizes has been obtained (Figs 7(D) and 4(B) respectively.) The distribution of tree sizes is not available for BCI, but some other tropical rainforests are known to have this property [20]. The biomass displays in the model a self-similar spatial distribution. In Fig. 7(E) the distribution of tree sizes is plotted together with new distributions at different scales. A standard space renormalization has been used.

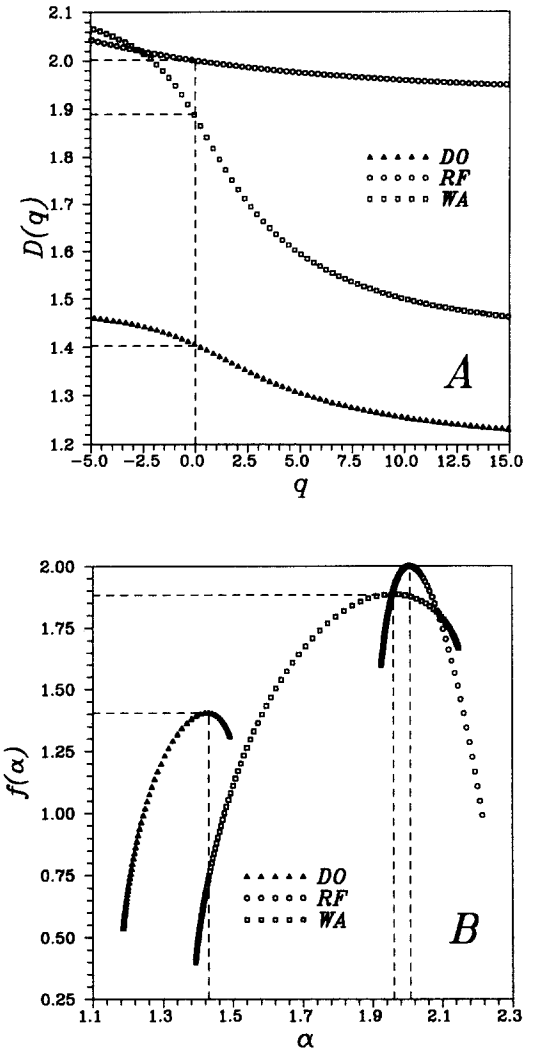

Fig. 9. Multifractal functions obtained for different sets of parameters. DO—damped oscillations; RF—random forest; WA—white area. The maximum spreading of these functions is found in the complex forest domain and close to it. It is a measure of the diversity generated by the system. The wider the spectra, the higher the amount of sizes available in the system.

The size of adjacent trees in a square $L \times L$ has been averaged to form the new block variable, and the resulting distribution has been properly rescaled:

$$S(k, l) = \frac{1}{L^2} \sum_{i,j=1}^{L} S(i, j) \tag{22}$$

$$F(L^2 S(k, l)) = F(S(i, j)), \tag{23}$$

where $k, l = 1, 2, \ldots N/L$ represent sites of the rescaled lattice and $F(S(i, j))$ and $F(S(k, l))$ are the original distribution and the new one, respectively. The comparison between the distributions points out the fractal distribution of biomass. An exact characterization of the critical transition that takes place would involve the determination of critical exponents. The rescaling performed over the distribution function sheds some light on the

question about what values those exponents would take. This subject will be further explored in future work.

4. SUMMARY AND DISCUSSION

In this paper we have analysed a tropical rainforest from the point of view of critical transitions in physics. Strong evidence of SOC have been found in the power-laws that the magnitudes of the system follow, both in space (multifractality, correlation function, clearings and tree sizes distributions) and time (biomass fluctuations). Since observational data are insufficient, we have presented and analysed a new model of forest dynamics. If the real rainforest really evolves close to a critical point, its physics should be independent of the fine details. This is the clue to make models useful. The results obtained are valuable in themselves but, in addition, the model has been shown to reproduce almost exactly some key characteristics of a real tropical rainforest. It is our belief that BCI is a system evolving at the edge of chaos. A rainforest is not a very ordered system, it does not behave periodically in space, nor in time. On the other hand, it is not a completely disordered system, with random spatial and temporal patterns. It just seems to poise itself to a self-organized critical state, where self-similarity is the rule, not the exception. This might be the configuration where the system is more robust against perturbations: any influence is already considered in the actual state of the system, and it would easily adapt to the real configuration. There is a fact that leads us to think in such a way. There were a few very large clearings in BCI that the model does not reproduce. They are very likely due to external disturbances (the plot of BCI of Fig. 1(A) was done after an El Niño episode). But when the spatial correlation function was carried out, a linear fitting of the results for small distances was obtained. The closest neighbour correlations have a very important contribution coming from these biggest clearings. Hence, although they do not adjust exactly to the size scaling function $N(G)$, they follow a power-law in the correlation function, while the results from the model display a small concavity in $C(d)$ for the smallest distances. External added disturbances in the system will be a future field of research, and perhaps the forest game will prove useful in the determination of how human influences should be introduced [21].

Not only the multifractal spectra, clearing distribution and spatial correlation function of BCI have been recovered, but some predictions about biomass fluctuations and tree distribution have been made. These predictions are coherent with what one would expect from a critical system. The observed properties of rainforests can therefore emerge from very simple interaction rules. It would be very interesting to know if rainforests move to the critical point when left to free evolution in any configuration, and are only led by the given rules [21].

Acknowledgements—The authors would like to thank R. Margalef, J. Bascompte, B. Luque, J. Delgado, J. Mach, J. Silvertown and J. Martí i Ruiz.

REFERENCES

1. H. E. Stanley, S. V. Buldyrev, A. L. Goldberger, Z. D. Goldberger, S. Havlin, R. N. Mantegna, S. M. Ossadnik, C. -K. Peng and M. Simmons, *Physica A* **205**, 214 (1994).
2. P. Bak, K. Chen and C. Tang, *Physica D* **38**, 5 (1989).
3. P. Bak, K. Chen and M. Creutz, *Nature* **342**, 780 (1989).
4. P. Bak and K. Chen, *Phys. Lett. A* **147**, 297 (1990).
5. S. A. Kauffman, *Physica D* **42**, 135 (1990).
6. L. Kadanoff, S. Nagel, L. Wu and S. Zhou, *Phys. Rev. A* **39**, 6524 (1989); A. Sornette and D. Sornette, *Europhys. Lett.* **9**, (1989) 197.

7. P. Bak and K. Sneppen, *Phys. Rev. Lett.* **71**, 4087 (1993); P. Bak and M. Paczuski, *Proc. Natl. Acad. Sci. USA* in press.
8. R. V. Solé and S. C. Manrubia, *J. Theor. Biol.* **173**, 31–40 (1995); R. V. Solé and S. C. Manrubia, *Phys. Rev. E* **51**, 6250 (1995).
9. T. C. Halsey, M. H. Jensen, L. P. Kadanoff, I. Procaccia and B. I. Shraiman, *Phys. Rev. A* **33**, 1141 (1986).
10. T. Nagatani, *Phys. Rev. E* **47**, 63 (1993).
11. T. R. Nelson, *Physica D* **55**, 69 (1992).
12. H. G. E. Hentschel and I. Procaccia, *Physica D* **8**, 435 (1983); C. Grebogi, E. Ott and J. E. Yorke, *Phys. Rev. A* **37**, 1711 (1988).
13. R. Cawley and R. D. Mauldin, *Adv. in Math.* **92**, 196 (1992).
14. C. W. Welden, S. W. Hewett, S. P Hubbell and R. B. Foster, *Ecology* **72**, 35 (1991).
15. T. C. Withmore, *An Introduction to Tropical Rainforests.* Clarendon Press, Oxford (1990).
16. J. P. Rigaut, *Fractals. Non-integral Dimensions and Applications*, Chapter 14. John Wiley & Sons, Chichester (1991).
17. L. V. Meisel, M. Johnson and P. J. Cote, *Phys. Rev. A* **45**, 6989 (1992); A. Block, W. von Bloh and H. J. Schellnhuber, *Phys. Rev. A* **42**, 1869 (1990).
18. H. Atmanspacher, H. Scheingraber and G. Wiedenmann. *Phys. Rev. A* **40**, 3954 (1989).
19. R. O. Lawton and F. E. Putz *Ecology* **69**, 764 (1988).
20. D. Lieberman, M. Lieberman, R. Peralta and G. S. Hartshorn *J. Ecol.* **73**, 915 (1985).
21. R. V. Solé and S. C. Manrubia, in preparation.